Kinetic Investigation of the Reactions of Mg(^{1}S), Ca(^{1}S), and Sr(^{1}S) Atoms with NO_2 over the Temperature Ranges 303−836, 303−916, and 303−986 K, Respectively

Chris Vinckier,* Joëlle Helaers, Piet Christiaens, and Jan Remeysen

Department of Chemistry, KU Leuven, Celestijnenlaan 200F, 3001 Heverlee, Belgium

Received: June 21, 1999; In Final Form: August 30, 1999

The kinetics of the second-order reactions $Mg(^1S) + NO_2(X^2A_1) \xrightarrow{k_{1_{Mg}}} MgO + NO$, $Ca(^1S) + NO_2(X^2A_1) \xrightarrow{k_{1_{Ca}}} CaO + NO$, and $Sr(^1S) + NO_2(X^2A_1) \xrightarrow{k_{1_{Sr}}} SrO + NO$ have been investigated in a fast-flow reactor in the temperature ranges of, respectively, 303−836, 303−916, and 303−986 K. Solid magnesium, calcium, and strontium pellets were thermally evaporated to generate the corresponding alkaline earth metal atoms in the gas phase. Their decays as a function of the added NO_2 concentration were followed by means of atomic absorption spectroscopy (AAS) at 285.2 nm for magnesium, 422.7 nm for calcium, and 460.7 nm for strontium atoms. All reactions show an Arrhenius behavior and the rate constants are given by $k_{1_{Mg}} = [(1.4 \pm 0.2) \times 10^{-11}] \exp(-3.4 \pm 0.6 \text{ kJ mol}^{-1}/RT)$ cm^3 molecule^{-1} s^{-1}, $k_{1_{Ca}} = [(1.5 \pm 0.6) \times 10^{-9}] \exp(-2.9 \pm 1.2 \text{ kJ mol}^{-1}/RT)$ cm^3 molecule^{-1} s^{-1}, and $k_{1_{Sr}} = [(1.2 \pm 0.1)\text{x } 10^{-9}] \exp(-0.9 \pm 0.3 \text{ kJ mol}^{-1}/RT)$ cm^3 molecule^{-1} s^{-1}. The results will be discussed in terms of the electron jump mechanism. Since the Mg/NO_2 reaction is too slow to proceed via this mechanism, a classical oxygen atom abstraction is suggested. In the case of the Ca/NO_2 and the Sr/NO_2 reactions, the experimental rate constants are too high to be quantitatively explained by the classical electron jump mechanism. The modified electron jump mechanism which takes into account long distance forces between the reagents gives a better agreement with the experimental values.

Introduction

This study of the alkaline earth metal atom reactions with NO_2 forms part of a broader kinetic investigation of the reactions of these metals with several molecules such as O_2, N_2O, and Cl_2.[1−7] The reason for selecting these compounds is that each of the reactions with these molecules proceeds according to a different reaction mechanism.

Indeed the alkaline earth metal atom reactions with oxygen are third-order reactions showing a positive temperature dependence due to an energy barrier at the intersection of the covalent and ionic potential energy surface of the reacting species.[1−4,8,9] All of the very exothermic N_2O reactions show a relatively high activation energy, associated with the closed-shell character of both reaction partners.[8] The Cl_2 reactions are very fast and are explained in terms of the electron jump mechanism.[6] A fundamental question is now in how far the alkaline earth metal atom/NO_2 reactions, which also form a metal oxide, follow the same reaction dynamics as the N_2O reactions.

Kinetic data on the Mg(Ca,Sr)(^{1}S)/NO_2 reactions are very scarse. The only kinetic measurements available have been measured in flames in the narrow temperature ranges between 873 and 1100 K.[10] All rate constants show a negative temperature dependence as can be seen in the following expressions:

$$k_{1_{Mg}} = [(6.6 \pm 0.5) \times 10^{-8}]T^{-1.65 \pm 0.03} \text{ cm}^3 \text{ molecule}^{-1} \text{ s}^{-1} \quad (1)$$

$$k_{1_{Ca}} = [(3.2 \pm 1.2) \times 10^{-8}]T^{-1.65 \pm 0.08} \text{ cm}^3 \text{ molecule}^{-1} \text{ s}^{-1} \quad (2)$$

$$k_{1_{Sr}} = [(2.5 \pm 0.5) \times 10^{-11}]T^{-0.78 \pm 0.02} \text{ cm}^3 \text{ molecule}^{-1} \text{ s}^{-1} \quad (3)$$

Another source of information on the Mg(Ca,Sr)/NO_2 reactions is coming from molecular beam experiments. Zare et al.[11,12] investigated the luminescence originating from the alkaline earth metal atom/NO_2 reactions in the visible wavelength region. While the Mg/NO_2 reaction did not show any detectable chemiluminescence, the Ca(Sr)/NO_2 reactions showed a broad continuum which has been assigned to the emission of a not well-characterized polyatomic species. This emitting species might be formed in several consecutive collisions between the vibrational excited ground-state metal oxide molecules or with NO_2. Total reaction cross sections for the Ca(Sr)/NO_2 reactions of, respectively, 93 and 127 Å^2 have been derived.[12] These values were considered to be in quantitative agreement with the values calculated in this work (see Discussion section). Herm et al.[13] also studied the Ca(Sr)/NO_2 reactions by means of a crossed beam technique. A "forwardly" orientated product distribution was observed, indicating that the reaction proceeds via a direct mechanism and not via a long-living complex. The fact that most of the observed wide angle scattering was due to reactive events indicated qualitatively that the cross sections for the Ca(Sr)/NO_2 reactions were large, in agreement with the results of Zare et al.[12] Contrary to the findings mentioned above, where a direct mechanism for the Ba(Ca,Sr)/NO_2 reactions was postulated, Parrish and Herm[14] predicted an electron jump mechanism. This mechanism has been invoked to explain the large cross sections of the alkali metal/halogen reactions,[15] in which the metal atom throws out its valence electron which is then captured by the halogen molecule. In this case, the reaction occurs without a classic collision between the reagents. However, the NO_2^- ion formed will not dissociate under the influence of the Me^+ field (Me = metal), implying that the intermediate $Me^+NO_2^-$ complex remains relatively stable. In the most recent crossed beam study of Davis et al.,[16] both reaction channels

10.1021/jp9920500 CCC: $18.00
Published on Web 12/07/1999

have been put forward for the Ba/NO_2 reaction: the first and most important one proceeds through a long-living Ba^+/NO_2^- complex, resulting from an electron transfer from the Ba atom toward the NO_2 molecule via the electron jump mechanism; in the second one, an oxygen abstraction occurs via a direct mechanism, leading to BaO in an electronic excited state. In this context, it needs to be pointed out that, in analogy with the alkaline earth metal atom/N_2O reactions, the metal oxides in the Mg(Sr)/NO_2 reactions can be formed in different electronic states. As will be illustrated in the Discussion section for the Mg/NO_2 reaction, the ground state ($X^1\Sigma^+$) as well as the triplet excited state ($^3\Pi$) is energetically accessible while for the Sr/NO_2 reaction SrO can be formed in the $X^1\Sigma^+$, $a^3\Pi$, and $A'^1\Pi$ states. The Ca/NO_2 reaction can only lead to the $X^1\Sigma^+$ ground state of CaO. In view of the possible occurrence of different reaction channels, one might expect a non-Arrhenius behavior, as has been observed for the Ca(Sr)/N_2O reactions.[7,8]

Kinetic measurements on the Mg(^{1}S), Ca(^{1}S), and Sr(^{1}S) atom/NO_2 reactions will now be presented covering the temperature ranges from, respectively, 303 to 836 , 303 to 916, and 303 to 986 K. The experiments were carried out in a fast-flow reactor using AAS as the detection technique for the thermally evaporated alkaline earth metal atoms. The results will be discussed in terms of the electron jump mechanism.

Experimental Technique

The experimental setup has been amply described in earlier publications,[2−6] and only a brief summary will be presented here. It consists of two major parts: a fast-flow reactor under low pressure and an AAS detection technique. The reactor is a quartz tube with an internal diameter of 5.7 cm and a length of 100 cm. At the upstream end the sample holder contained the metal pellets which were thermally evaporated at 600−700 K by means of a kanthal resistance wire. By means of the carrier gas helium, the alkaline earth metal atoms were transported downstream in the kinetic zone where they were mixed with an excess of NO_2. In the pressure range from 6 to 12 Torr, the flow velocity v_g of the carrier gas helium has a constant value of 320 ± 10 cm s^{-1} at 303 K. The temperature in the kinetic zone could be varied between 303 and 1000 K by means of an oven, and the temperature was monitored by a chromel−alumel thermocouple. Magnesium, calcium, and strontium atoms were detected by AAS at, respectively, 285.2, 422.7, and 460.7 nm.

Assuming that the detection limit corresponds to an absorbance of $A = 0.005$, one can calculate the detection limit for the Mg(Ca,Sr) atoms by using a formalism explained in an earlier paper,[17] $[Mg(Ca,Sr)] = C_1AL^{-1}T_g^{1/2}$, in which C_1 is a proportionality constant, L the optical path length (5.7 cm), and T_g the gas temperature. With values for $C_1(Mg) = 1.820 \times 10^{10}$ cm^{-2} $K^{-1/2}$, $C_1(Ca) = 0.663 \times 10^{10}$ cm^{-2} $K^{-1/2}$, and $C_1(Sr) = 0.428 \times 10^{10}$ cm^{-2} $K^{-1/2}$ at 500 K,[18] one can calculate the following detection limits: for magnesium, 3.6×10^8 atoms cm^{-3} or 3.11 ppb; for calcium, 1.3×10^8 atoms cm^{-3} or 1.12 ppb; for strontium, 8.4×10^7 atoms cm^{-3} or 0.72 ppb at 6 Torr and 500 K.

Minimum distances between the metal atom source, the NO_2 inlet, and the kinetic zone were maintained to allow for sufficient mixing of the reagents.[5,6] Kinetic measurements were made by following the decay of the alkaline earth metal atom absorbance as a function of the axial distance along the fast-flow reactor. This was realized by moving the entire reactor assembly along its axis relative to the detection equipment which remained at a fixed position. Decays of the absorbances as a function of the distance can easily be transformed into decays as a function of the reaction time t using the expression $t = z_d/v_g$. An advantage of this technique is that relative positions of the metal atom source and the NO_2 inlet remain constant during the experiments. Reproducible absorbances could be maintained within 10% when the temperature T_s of the metal pellets was stabilized within ±1%.

For all the investigated reactions helium (L'Air Liquide) with a purity of 99.995% was used as a carrier gas as well as in the gas mixtures. The nitrogen dioxide concentrations were equal to 0.92% and 0.117% of NO_2 for the Mg/NO_2 reaction, 0.117% of NO_2 for the Ca/NO_2 reaction, and 0.1% of NO_2 for the Sr/NO_2 reaction. The magnesium pellets (Alfa Products), the calcium pellets (Fluka), and the strontium pellets (Aldrich), respectively, had a purity of about 99.8%, 99.5%, and 99.0%.

As will be pointed out in the next section, adding a mixture with low NO_2 content may lead to rather unstable NO_2 flows and this in view of possible wall adsorption phenomena in the gas flow controllers, stainless steel and Teflon tubing, etc.

Weighted regressions on all plots were made using the statistical SAS package.[19] The quoted errors σ were the standard deviations.

Results

Determination of the Rate Constants $k_{1_{Mg}}$, $k_{1_{Ca}}$, and $k_{1_{Sr}}$. The kinetic formalism used in the derivation of the rate constants of the Mg(Ca,Sr) + NO_2 reactions has already been described in previous papers,[5,6]

$$\ln A_{Mg(Ca,Sr)} = -\left\{\frac{k_{1_{Mg(Ca,Sr)}}[NO_2]}{\eta} + \frac{7.43D_{Mg(Ca,Sr)/He}}{2r^2}\right\}t + B \quad (4)$$

in which $\ln A_{Mg(Ca,Sr)}$ is the natural logarithm of, respectively, the magnesium, calcium, and strontium absorbance, η is a correction factor depending on the flow characteristics, $D_{Mg(Ca,Sr)/He}$ is the binary diffusion coefficient of the Mg, Ca, and Sr atoms in the carrier gas helium, r is the reactor radius, t is the reaction time, and B is an integration constant. The correction factor η is related to the flow characteristics, and the determination of its magnitude has been amply discussed elsewhere.[20]

The use of eq 4 for obtaining kinetic parameters has been well-illustrated in our earlier work[5,21] and will only briefly be summarized here.

The values of $k_{1_{Mg(Ca,Sr)}}$ were determined by following first $\ln A_{Mg(Ca,Sr)}$ as a function of the reaction time t at various amounts of NO_2 added. A weighted linear regression of $\ln A_{Mg(Ca,Sr)}$ versus t was carried out using a statistical error for $\ln A_{Mg(Ca,Sr)}$ which at average varies between 9 and 11% going from the highest to the lowest value of $\ln A_{Mg(Ca,Sr)}$. As an example the pseudo-first-order decays of Ca(^{1}S) atoms as a function of the reaction time t for various initial NO_2 concentrations at a temperature $T_g = 303$ K and a pressure P_r equal to 10 Torr are shown in Figure 1.

In the next step the slopes S of these lines were plotted versus the added $[NO_2]$ and a weighted linear regression results in a straight line with a slope directly equal to $k_{1_{Mg(Ca,Sr)}}/\eta$ as is illustrated in Figures 2−4 for three different temperatures: 303, 665, and 836 K for the Mg/NO_2 reaction; 303, 615, and 916 K for the Ca/NO_2 reaction; 303, 662, and 952 K for the Sr/NO_2 reaction.

When the magnitude of the intercept is larger than 2 times its standard deviation but smaller than $7.34D_{Mg(Ca,Sr)/He}/2r^2$, plug-flow conditions do not prevail and the factor η is set equal to 1.3 with an associated systematic error of 10%.[20] In the other

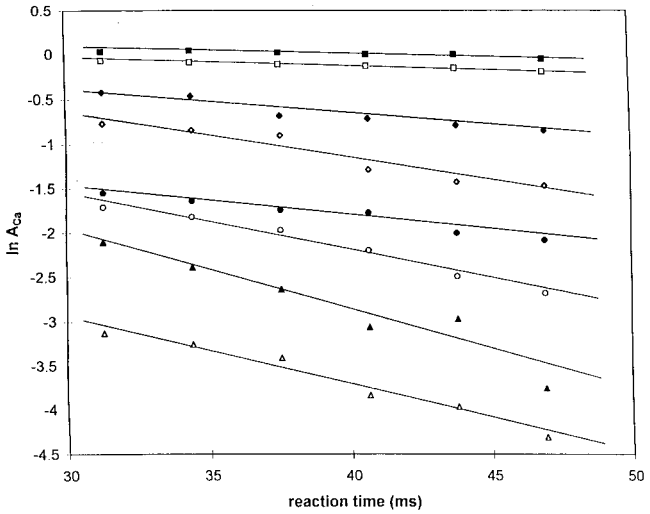

Figure 1. natural logarithm of the Ca atom absorbance as a function of the reaction time t with various amounts of added NO_2. The experimental conditions are $T_g = 303$ K, $P_r = 10$ Torr, He as carrier gas; [NO_2] (■) 0; (□) 0; (◆) 12.0; (◇) 18.4; (●) 24.8; (○) 31.2; (▲) 37.8; (△) 44.1 expressed in units of 10^{10} molecules cm^{-3}.

cases, when the magnitude of the intercept is about equal to $7.34D_{Mg(Ca,Sr)/He}/2r^2$, a correction factor of 1.6 will be used. The uncertainties σ_S and σ_k for the calculated values of the slope S and the rate constants $k_{1_{Mg(Ca,Sr)}}$ were calculated by combining the uncertainties of several variables such as the temperature, flow velocity, and total pressure as well as of the dimension of the reactor radius according to the method explained in detail by Howard.[22] When the correction factor 1.3 was used, the systematic error of 10% was taken into account resulting in the total standard deviation σ_k. Finally, the observed slopes in Figures 2−4 need to be multiplied by η to obtain the correct second-order rate constants $k_{1_{Mg(Ca,Sr)}}$. In the examples mentioned above, second-order rate constants $k_{1_{Mg}} = 3.8 \pm 0.4$ (at 303 K), 6.7 ± 2.1 (at 665 K), and 15.8 ± 3.4 (at 836 K) in units of 10^{-12} cm^3 $molecule^{-1}$ s^{-1} were derived. In the examples for the Ca/NO_2, reaction rate constants $k_{1_{Ca}} = 2.1 \pm 0.4$ (at 303 K), 11.0 ± 2.0 (at 615 K), and 8.7 ± 1.6 (at 916 K) in units of 10^{-10} cm^3 $molecule^{-1}$ s^{-1} were obtained. Finally for the Sr/NO_2 reaction values for $k_{1_{Sr}}$ were equal to 7.8 ± 1.1 (at 303 K), 9.3 ± 1.4 (at 662 K), and 11.6 ± 0.4 (at 952 K) in units of 10^{-10} cm^3 $molecule^{-1}$ s^{-1}.

To confirm the second-order behavior of the reactions, the pressure dependence of the rate constants $k_{1_{Mg(Ca,Sr)}}$ was examined in the range between 6 and 12 Torr. It was noticed that at various temperatures between 303 and 748 K $k_{1_{Mg(Ca,Sr)}}$ was independent of the pressure. These experiments also confirm that hydrodynamic effects, as there are the mixing of the reagents or the wall-loss of Mg(Ca,Sr) atoms, have no systematic effect on the derived values of the rate constants.

Furthermore, the influence of the initial alkaline earth metal atom concentration on the value of $k_{1_{Mg(Ca,Sr)}}$ has been checked. For this purpose, $A^i_{Mg(Ca,Sr)}$ was varied with a factor of 2−5 and in none of the cases any systematic effect on $k_{1_{Mg(Ca,Sr)}}$ has been observed. This proves that, as expected at these low initial metal atom concentrations, mutual reactions between the metal atoms or consecutive reaction steps involving these metal atoms were unimportant.

Temperature Dependence of $k_{1_{Mg}}$, $k_{1_{Ca}}$, and $k_{1_{Sr}}$. The experimental conditions together with all the values of $k_{1_{Mg}}$, $k_{1_{Ca}}$, and $k_{1_{Sr}}$ determined in the temperature ranges of, respectively, 303−836, 303−916, and 303−986 K are listed in Table 1. Some attention has to be paid to the fact that the variation in the values of some individual rate constants measured at a constant temperature is much larger than stated by their standard deviations. In this context, it has to be mentioned that in our recent kinetic studies of the reactions between metal atoms and other additives such as oxygen, nitrous oxide, methyl halides, etc., this variation of the rate constants was smaller and in much better agreement with the stated standard deviations.[4,7,23] While carrying out the experiments with NO_2 as additive gas, it has been noticed that the quality of the decay curves is much lower than in the case of the other additives. Sometimes a lower metal atom decay was observed at presumably a higher but incorrectly setted NO_2 concentration, as is, e.g., the case in Figure 1; the slope of ln A as a function of t is smaller at the NO_2 concentration of 2.48×10^{11} molecules cm^{-3} than at 1.84×10^{11} molecules cm^{-3}. This can most probably be explained by unstable NO_2 flows at these low concentrations, due to adsorption phenomena on various wall surfaces of the whole gas flow system.

These results can be fitted to the Arrhenius formalism according to eq 5,

$$k_{1_{Mg(Ca,Sr)}} = A \exp\left(\frac{-E_a}{RT}\right) \tag{5}$$

in which A is the pre-exponential factor (cm^3 $molecule^{-1}$ s^{-1}), E_a is the activation energy (kJ mol^{-1}), R is the universal gas constant (8.31 J mol^{-1} K^{-1}), and T is the temperature (K).

When the rate constants $k_{1_{Mg(Ca,Sr)}}$ were fitted to eq 5 by means of a weighted nonlinear regression using the SAS package,[19] the following Arrhenius expressions were obtained:

$$k_{1_{Mg}} = [(1.4 \pm 0.2) \times 10^{-11}] \times \exp\left(\frac{-3.4 \pm 0.6 \text{ kJ mol}^{-1}}{RT}\right) \text{cm}^3 \text{ molecule}^{-1} \text{ s}^{-1} \tag{6}$$

$$k_{1_{Ca}} = [(1.5 \pm 0.6) \times 10^{-9}] \times \exp\left(\frac{-2.9 \pm 1.2 \text{ kJ mol}^{-1}}{RT}\right) \text{cm}^3 \text{ molecule}^{-1} \text{ s}^{-1} \tag{7}$$

$$k_{1_{Sr}} = [(1.2 \pm 0.1) \times 10^{-9}] \times \exp\left(\frac{-0.9 \pm 0.3 \text{ kJ mol}^{-1}}{RT}\right) \text{cm}^3 \text{ molecule}^{-1} \text{ s}^{-1} \tag{8}$$

The quoted error margins on both the pre-exponential factors and the Arrhenius activation energies are at the 1σ level.

The values of ln $k_{1_{Mg(Ca,Sr)}}$ from Table 1 are shown versus $1/T$ in Figure 5.

One sees that for all the reactions the rate constants slightly increase with the temperature, implying the presence of a small or even negligible activation energy.

It should be pointed out here that for the calculation of the Arrhenius parameters of the Ca/NO_2 reaction only the weighted average value of 2.6×10^{-10} cm^3 $molecule^{-1}$ s^{-1} at 303 K was used in view of the large scatter on the data and the unreasonably high weight of the large number of measurements at 303 K. Indeed when all the individual values were fitted to the Arrhenius formalism, including the eight measurements at 303 K, an Arrhenius activation energy of 5.0 ± 1.0 kJ mol^{-1} was obtained, which is about 70% higher than our value of 2.9 ± 1.2 kJ mol^{-1}. When the same procedure was applied to the Mg/NO_2 and the Sr/NO_2 reactions, the calculated Arrhenius

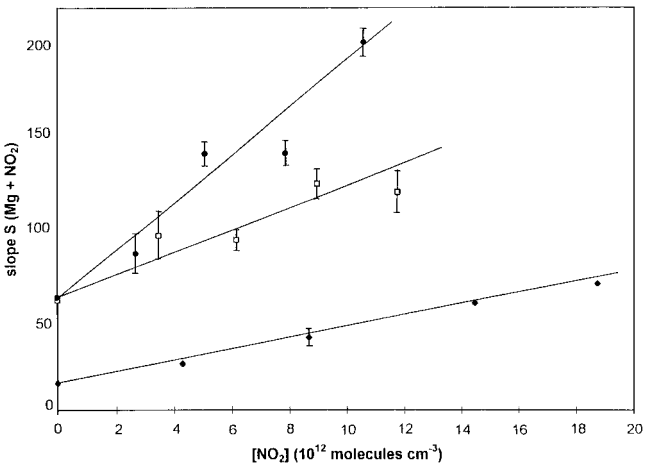

Figure 2. Slopes S of eq 4 for the Mg/NO_2 reaction as a function of the added NO_2 concentration. The experimental conditions are T_g = 303 K (◆) (P_r = 8 Torr); 665 K (□) (P_r = 12 Torr); 836 K(●) (P_r = 8 Torr), He as carrier gas, $[NO_2]$ is expressed in units of 10^{12} molecules cm^{-3}.

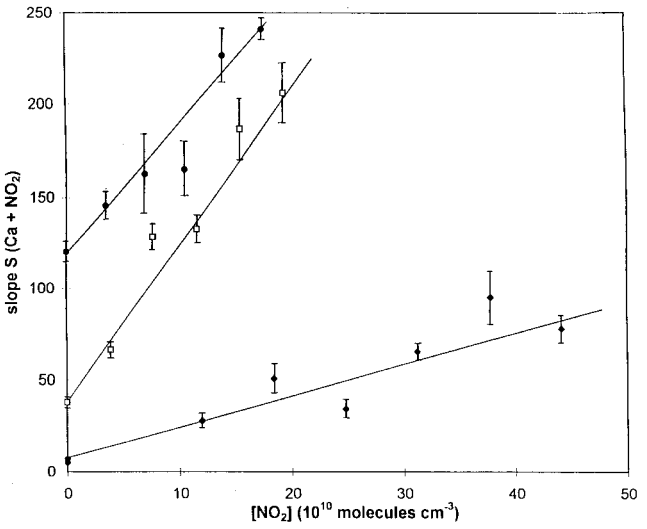

Figure 3. Slopes S of eq 4 for the Ca/NO_2 reaction as a function of the added NO_2 concentration. The experimental conditions are T_g = 303 K (◆) (P_r = 10 Torr); 615 K (□) (P_r = 10 Torr); 916 K (●) (P_r = 8 Torr), He as carrier gas, $[NO_2]$ is expressed in units of 10^{10} molecules cm^{-3}.

parameters fell within the error margins quoted in eqs 6 and 8.

One sees that all the reactions are characterized by a small or even negligible activation energy in the range between 0.9 and 3.4 kJ mol^{-1} and a relatively high pre-exponential factor, which is quantitatively in line with the large cross sections determined in molecular beam experiments.[12]

Discussion

The reaction products of the exothermic $Mg(Ca,Sr)/NO_2$ reactions are summarized in Table 2.[24]

From Table 2, one sees that the Ca/NO_2 reaction can only lead to ground-state CaO ($X^1\Sigma^+$), while MgO and SrO can be formed in different electronically excited states. However, it needs to be pointed out that MgO($^3\Pi$) and SrO($a^3\Pi$) are spin-forbidden reaction products. Since a clear Arrhenius behavior is observed for all three reactions, the possible occurrence of two reaction channels with different activation energies is not likely.

If one compares the reaction enthalpies from Table 2 with those of the analogous alkaline earth metal atom/N_2O reactions,[24] it becomes clear that the NO_2 reactions are far less exothermic. The reason for the higher exothermicity of the alkaline earth metal atom/N_2O reactions is the low bond energy $D_0(N_2-O)$ of the O atom in the N_2O molecule. This value is about equal to 162 kJ mol^{-1}, which is indeed much lower than the bond energy of the analogous NO_2 molecule, i.e., 310 kJ mol^{-1}.[24]

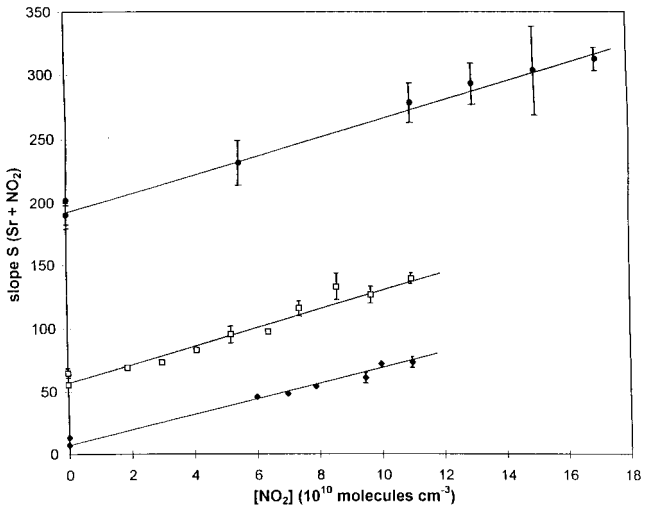

Figure 4. Slopes S of eq 4 for the Sr/NO_2 reaction as a function of the added NO_2 concentration. The experimental conditions are T_g = 303 K (◆) (P_r = 10 Torr); 662 K (□) (P_r = 10 Torr); 952 K (●) (P_r = 8 Torr), He as carrier gas, $[NO_2]$ is expressed in units of 10^{10} molecules cm^{-3}.

The measured rate constants in this work can only be compared with the values of Kashireninov et al., derived in the narrow temperature ranges between 873 and 1100 K.[10] Equations 1−3 all show a small negative temperature dependence, which for $k_{1_{Mg}}$ and $k_{1_{Ca}}$ is given by the factor $T^{-1.65}$ and for $k_{1_{Sr}}$ by the factor $T^{-0.78}$. However, in this narrow temperature range, the values of the rate constants will only decrease with about 20% going from 873 to 1100 K. If this calculation is repeated in this same narrow temperature range using our values of $k_{1_{Mg(Ca,Sr)}}$ from eqs 6−8, the rate constants will increase with less than 10%. So the effect of the temperature on the values of the rate constants is far less than one might think on the basis of the kinetic expressions. However, if one compares the absolute magnitude of the rate constants at the highest temperatures covered in our work, one sees a very large difference as is shown in Table 3.

The values of $k_{1_{Mg(Ca,Sr)}}$ are compared at temperatures of 836, 916, and 986 K for, respectively, the Mg, Ca, and Sr/NO_2 reaction. One can see that all our values and especially those of the Ca and Sr/NO_2 reactions are much larger. It should be pointed out here that the determination of kinetic data from flame studies by means of the TVDF (temperature variation of the diffusion flame) technique[10] is strongly complicated through several interferences as there are the high-temperature gradients in the reaction zone, the occurrence of secondary reactions, and the influence of condensation of the gas phase products onto the thermocouples.

Our data also allow calculation of the reaction cross sections Q_r for the $Mg(Ca,Sr)/NO_2$ reactions at 303 K as well as at the highest temperature covered. These values are compared with the cross sections due to reactive processes, obtained from molecular beam experiments[12] (see Table 4).

From Table 4, it becomes clear that the values of Q_r calculated from our kinetic constants are in line with those obtained from molecular beam experiments.

TABLE 1: Rate Constants $k_{1_{Mg(Ca,Sr)}}$ of the Reactions $Mg(^1S) + NO_2$, $Ca(^1S) + NO_2$, and $Sr(^1S) + NO_2$ as a Function of the Temperature T_g[a]

T_g (K)	P_r (Torr)	A^i_{Mg}	$k_{1_{Mg}}$ ($\times 10^{-12}$ cm^3 molecule^{-1} s^{-1})	T_g (K)	P_r (Torr)	A^i_{Ca}	$k_{1_{Ca}}$ ($\times 10^{-10}$ cm^3 molecule^{-1} s^{-1})	T_g (K)	P_r (Torr)	A^i_{Sr}	$k_{1_{Sr}}$ ($\times 10^{-10}$ cm^3 molecule^{-1} s^{-1})
303	8	0.17	3.8 ± 0.4	303	8	0.46	2.2 ± 0.3	303	6	0.09	9.0 ± 0.9
303	8	0.22	3.1 ± 0.1	303	8	0.66	2.5 ± 0.5	303	8	0.50	6.0 ± 0.9
303	8	0.22	3.0 ± 0.5	303	8	0.54	2.4 ± 0.4	303	9	0.34	10.3 ± 1.4
303	8	0.32	3.2 ± 0.7	303	10	0.19	3.2 ± 0.6	303	9	0.25	9.4 ± 1.5
386	8	0.20	3.6 ± 0.4	303	10	0.87	2.5 ± 0.4	303	10	0.31	7.8 ± 1.1
390	8	0.45	4.9 ± 0.3	303	10	0.97	2.1 ± 0.4	303	11	0.23	6.2 ± 0.7
400	8.5	0.54	5.9 ± 0.4	303	12	0.25	4.7 ± 0.7	303	12	0.42	11.8 ± 0.9
478	7	0.37	7.9 ± 0.4	303	12	0.30	3.2 ± 0.5	357	8	0.25	7.7 ± 1.4
481	8	0.25	3.8 ± 0.5	381	12	0.14	8.5 ± 0.3	407	8	0.35	9.6 ± 0.4
482	8	0.42	8.6 ± 1.0	388	10	0.67	8.7 ± 1.2	454	8	0.39	7.3 ± 1.1
544	6	0.45	11.3 ± 1.8	390	8	0.29	3.6 ± 0.6	499	8	0.25	10.4 ± 0.7
550	6	0.45	10.2 ± 1.4	390	10	0.11	6.6 ± 1.1	508	8	0.73	10.8 ± 0.2
550	6	0.58	7.5 ± 1.3	447	8	0.49	4.5 ± 0.6	508	8	0.21	11.5 ± 0.6
550	9	0.77	14.6 ± 2.2	456	10	0.57	8.7 ± 2.0	542	8	0.34	10.4 ± 0.7
550	9	0.70	12.0 ± 1.5	498	10	0.42	10.0 ± 2.0	662	6	0.28	9.4 ± 1.9
552	12	0.61	11.5 ± 1.6	509	8	0.27	5.4 ± 0.9	662	7	0.21	8.3 ± 1.3
552	12	1.05	12.2 ± 2.0	566	10	0.60	10.0 ± 2.0	662	8	0.08	9.2 ± 0.3
616	8	0.62	7.9 ± 1.0	576	8	0.28	8.4 ± 1.7	662	10	0.17	9.3 ± 1.4
620	8	0.21	8.5 ± 0.8	591	12	0.65	6.7 ± 1.0	662	12	0.42	8.6 ± 1.4
620	8	0.54	7.3 ± 0.3	602	8	0.14	11.0 ± 3.0	681	8	0.26	8.4 ± 1.0
665	6	0.10	6.7 ± 1.6	602	8	0.29	10.0 ± 3.0	764	8	0.31	11.9 ± 0.6
665	8	0.85	7.9 ± 2.7	615	10	0.53	11.0 ± 2.0	798	8	0.13	10.7 ± 0.3
665	10	0.10	7.6 ± 2.4	624	8	0.44	6.8 ± 1.7	798	8	0.51	10.3 ± 0.5
665	12	0.18	6.7 ± 2.1	700	12	0.18	17.0 ± 6.0	848	8	0.31	10.5 ± 1.0
748	6	0.60	8.2 ± 0.9	721	10	0.37	10.0 ± 2.0	893	8	0.19	12.5 ± 1.0
748	8	0.85	8.9 ± 0.3	736	8	0.56	10.0 ± 3.0	952	8	0.23	11.6 ± 0.4
748	10	0.96	6.9 ± 0.2	840	8	0.63	7.4 ± 3.1	986	8	0.16	11.7 ± 1.4
748	12	0.32	9.1 ± 3.9	916	8	0.27	8.7 ± 1.6				
833	8	1.10	15.9 ± 1.8								
836	8	0.60	15.8 ± 3.4								

[a] P_r Is the Reactor Pressure and $A^i_{Mg(Ca,Sr)}$ Are the Initial Absorbances

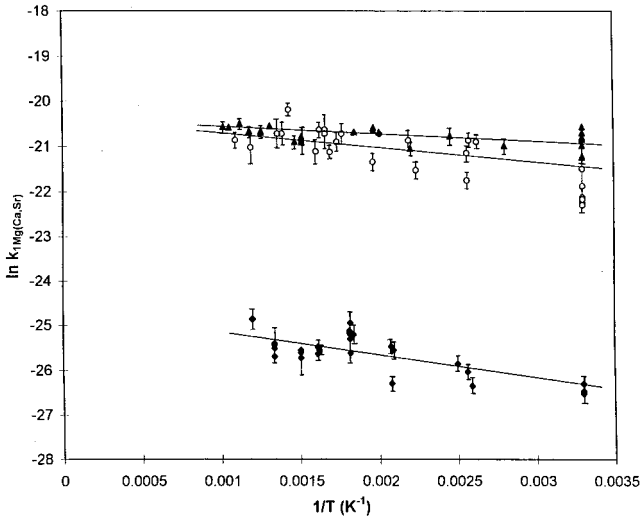

Figure 5. Plot of ln $k_{1_{Mg(Ca,Sr)}}$ versus $1/T$ according to the weighted nonlinear regression method: Mg/NO_2 (◆) (eq 6); Ca/NO_2 (○) (eq 7); Sr/NO_2 (▲) (eq 8).

From a mechanistic point of view, it is worthwhile to check if the alkaline earth metal atom/NO_2 reactions are governed by the electron jump mechanism. As already mentioned in the Introduction, a few authors have postulated this mechanism[14,16] in view of the large cross sections observed in molecular beam experiments.[12] According to this electron jump mechanism the rate constant k_{ej} for the reaction is given by eq 9,

$$k_{ej} = \pi r_c^{\,2} v_r \qquad (9)$$

in which v_r is the average molecular velocity, equal to $(8RT/\pi\mu)^{0.5}$, with μ the reduced mass of the reagents; r_c is the distance between the metal atom and NO_2 at which the electron jumps from the metal toward the NO_2 molecule. The value of r_c is given by[15]

TABLE 2: Reaction Enthalpy ΔH_R of the Exothermic Mg(Ca,Sr)/NO_2 Reactions Leading to Various Electronic States of the Corresponding Metal Oxide[24]

possible excited states of the metal oxide	ΔH_R (kJ mol^{-1})
$Mg(^1S) + NO_2(X^2A_1) \rightarrow MgO(X^1\Sigma^+) + NO(X^2\Pi)$	−31.8
$Mg(^1S) + NO_2(X^2A_1) \rightarrow MgO(^3\Pi) + NO(X^2\Pi)$	−4.2
$Ca(^1S) + NO_2(X^2A_1) \rightarrow CaO(X^1\Sigma^+) + NO(X^2\Pi)$	−76.7
$Sr(^1S) + NO_2(X^2A_1) \rightarrow SrO(X^1\Sigma^+) + NO(X^2\Pi)$	−120.2
$Sr(^1S) + NO_2(X^2A_1) \rightarrow SrO(a^3\Pi) + NO(X^2\Pi)$	−11.8
$Sr(^1S) + NO_2(X^2A_1) \rightarrow SrO(A'^1\Pi) + NO(X^2\Pi)$	−3.0

TABLE 3: Rate Constants on the Basis of Ref 10 (Eqs 1−3) and Our Values (Eqs 6−8), Both Calculated at the Highest Temperature Covered in Our Work

	highest T_{exp} (K) from our work	k_1 (Kashireninov) (cm^3 molecule^{-1} s^{-1})	k_1 (this work) (cm^3 molecule^{-1} s^{-1})
Mg	836	1.0×10^{-12}	8.6×10^{-12}
Ca	916	4.2×10^{-13}	1.0×10^{-9}
Sr	986	1.2×10^{-13}	1.0×10^{-9}

TABLE 4: Comparison between Our Calculated Values of the Cross Sections Q_r and the Values Obtained in Ref 12

	T (K)	Q_r (Å^2) (this work)	Q_r (Å^2) (ref 12)
Mg	303	0.5	
	836	1.5	
Ca	303	47.5	93
	916	91.5	
Sr	303	178.0	127
	986	140.8	

$$r_c = \frac{14.35}{IE_{Mg(Ca,Sr)} - EA_v(NO_2)}\ \text{Å} \qquad (10)$$

in which $IE_{Mg(Ca,Sr)}$ is the ionization energy of the Mg, Ca, or Sr atom, respectively, equal to 7.64, 6.10, and 5.69 eV, $EA_v(NO_2)$ is the vertical electron affinity of the NO_2 molecule. In the calculation of r_c performed by Zare et al.,[12] the value of 3.15 eV for $EA_v(NO_2)$ was selected,[25,26] while in our calculation the lower and more recent value of 2.36 eV[27,28] will be taken. The values for r_c of the Mg(Ca,Sr)/NO_2 reactions obtained from eq 10 are shown in Table 5.

In the next step, the values of the electron jump rate constants can be calculated at each temperature by means of eq 9 and can then be compared with the value of the experimental rate constant at the same temperature. Table 5 only shows the results at room temperature and at the highest experimental temperature. From Table 5, it is clear that the Mg/NO_2 reaction is far too slow to proceed according to the electron jump mechanism, and thus a classical oxygen atom abstraction mechanism is most likely. This is consistent with the higher ionization energy of the Mg atom compared to the Ca and Sr atoms. For the Ca/NO_2 reaction at room temperature, the experimentally determined rate constant seems to be in very good agreement with the predicted value on the basis of the electron jump mechanism. However, it should be pointed out that for all measurements at higher temperature, the electron jump rate constant is lower than the experimental value; for example, at the highest temperature of 916 K, the electron jump rate constant is even 50% lower than the experimentally observed value. This has also been seen for the Sr/NO_2 reaction over the entire temperature range. These larger experimental values might be explained by taking into account long-range forces between the reacting species.[29] These forces are mainly attractive dispersion forces which are active at distances larger than the electron jump distance. The long-range interaction is being controlled by the C_6/R^6 potential, which contains two components: a dispersion coefficient C_6^{disp} and a dipole-induced component C_6^{ind}:[30]

$$C_6 = C_6^{disp} + C_6^{ind} \qquad (11)$$

The dipole-induced component C_6^{ind} is given by eq 12,

$$C_6^{ind} = (\mu_{NO_2})^2 \frac{\alpha_{Ca(Sr)}}{(4\pi\epsilon_0)^2} \qquad (12)$$

in which μ_{NO_2} represents the permanent dipole moment of NO_2 ($=1.336 \times 10^{-30}$ Cm), $\alpha_{Ca(Sr)}$ is the polarizability of the metal atom, respectively, Ca ($=22.8 \times 10^{-30}$ m^3) and Sr ($=27.6 \times 10^{-30}$ m^3), and ϵ_0 is the permittivity in a vacuum ($=8.854 \times 10^{-12}$ C^2 J^{-1} m^{-1}). When these numbers are inserted into eq 12, one obtains values of C_6^{ind} for the Ca/NO_2 and the Sr/NO_2 reaction partners, respectively, equal to 3.6×10^{-19} J Å^6 molecule^{-1} and 4.4×10^{-19} J Å^6 molecule^{-1}.

The dispersion coefficient C_6^{disp} can be calculated on the basis of the London-expression,[30]

$$C_6^{disp} = \frac{3}{2}\alpha_{Ca(Sr)}\alpha_{NO_2}\frac{(IE_{Ca(Sr)}IE_{NO_2})}{(IE_{Ca(Sr)} + IE_{NO_2})} \qquad (13)$$

in which α_{NO_2} is the polarizability of NO_2 ($=3.0 \times 10^{-30}$ m^3),[31] $IE_{Ca(Sr)}$ and IE_{NO_2} are the ionization energies of Ca, Sr, and NO_2, respectively, equal to 589.5, 548.1, and 942.1 kJ mol^{-1}.[32] When C_6^{disp} is calculated from eq 13 values for the Ca/NO_2 and the Sr/NO_2 reactions, respectively, equal to 6.2×10^{-17} J Å^6 molecule^{-1} and 7.2×10^{-17} J Å^6 molecule^{-1} are obtained, which are much larger than the corresponding values of the induced dipole component C_6^{ind}.

TABLE 5: Comparison between the Calculated Values of r_c (eq 10), k_{ej} (eq 9), and k_{mej} (eq 14) with the Value of r_c(exp) Derived from k_{exp} and the Experimental Value k_{exp} at Room Temperature as well as At the Highest Temperature

	r_c (Å)	k_{ej} (cm^3 molecule^{-1} s^{-1})	r_c(exp) (Å)	k_{exp} (cm^3 molecule^{-1} s^{-1})	k_{mej} (cm^3 molecule^{-1} s^{-1})
Mg/NO_2 (303 K)	2.7	1.5×10^{-10}	0.4	3.2×10^{-12}	
Mg/NO_2 (836 K)	2.7	2.4×10^{-10}	0.7	15.8×10^{-12}	
Ca/NO_2 (303 K)	3.8	2.5×10^{-10}	3.9	2.6×10^{-10}	7.2×10^{-10}
Ca/NO_2 (916 K)	3.8	4.3×10^{-10}	5.4	8.7×10^{-10}	8.7×10^{-10}
Sr/NO_2 (303 K)	4.3	2.7×10^{-10}	7.5	8.2×10^{-10}	6.4×10^{-10}
Sr/NO_2 (986 K)	4.3	4.8×10^{-10}	6.7	11.7×10^{-10}	7.8×10^{-10}

According to the modified electron jump mechanism, the rate constant k_{mej} is given by eq 14,[33]

$$k_{mej} = \pi\left(\frac{2C_6}{RT}\right)^{1/3}\left(\frac{8RT}{\pi\mu}\right)^{1/2}\Gamma\,(2/3)\ \text{cm}^3\ \text{molecule}^{-1}\ \text{s}^{-1} \qquad (14)$$

in which Γ ($^2/_3$) is the gamma function of $^2/_3$ ($=1.354$), T is the gas temperature, R is the universal gas constant ($=1.38 \times 10^{-23}$ J molecule^{-1} K^{-1}), and μ is the reduced mass of the reacting species.

It needs to be pointed out that eq 14 is only valid when the following condition is fulfilled:

$$\frac{2C_6}{r_c^6} > RT \qquad (15)$$

in which the value of r_c is calculated by means of the classic electron jump mechanism (eq 10). When eq 15 is applied to the Ca/NO_2 and the Sr/NO_2 reactions, this condition is fulfilled at each temperature. The values of the rate constant k_{mej} are calculated by means of eq 14 over the entire temperature range, but only the values at room temperature and at the highest temperature are shown in Table 5. For the Ca/NO_2 reaction at 303 and 916 K, the value of k_{mej} is, respectively, equal to 7.2×10^{-10} cm^3 molecule^{-1} s^{-1} and 8.7×10^{-10} cm^3 molecule^{-1} s^{-1}. One notices that k_{mej} at 303 K is much higher than the experimental value, while k_{mej} at 916 K is in perfect agreement with the experimental value. However, if one checks the rate constants over the entire temperature range, the general trend for the Ca/NO_2 reaction is that, except for a few values at 390, 447, 509, and 700 K, all the other rate constants lie in the range from 6.6×10^{-10} to 11×10^{-10} cm^3 molecule^{-1} s^{-1}. This is in fairly good agreement with the values between 7.2×10^{-10} and 8.7×10^{-10} cm^3 molecule^{-1} s^{-1} calculated on the basis of the modified electron jump model (see Table 5).

In the case of the Sr/NO_2 reaction at 303 and 986 K k_{mej} is respectively equal to 6.4×10^{-10} cm^3 molecule^{-1} s^{-1} and 7.8×10^{-10} cm^3 molecule^{-1} s^{-1}. For the Sr/NO_2 reaction one can notice that the rate constants predicted by the modified electron jump mechanism over the entire temperature range also approach the experimental values much more than the values on the basis of the classical electron jump mechanism, but apparently this modified electron jump mechanism still slightly underestimates k_{1Sr}.

It needs to be pointed out here that the electron jump or modified electron jump mechanisms imply the absence of an energy barrier,[15] which is in agreement with the very low Arrhenius activation energies of 2.9 ± 1.2 and 0.9 ± 0.3 kJ mol^{-1} for, respectively, the Ca/NO_2 and the Sr/NO_2 reactions. These small barriers are thought to be due to the closed-shell configuration of the alkaline earth metal atoms with two paired electrons on the outermost orbital.

Acknowledgment. We thank the Fund for Joint Basic Research (FKFO), Brussels, Belgium, for a research grant. C.V. is a Research Director of the National Fund for Scientific Research (Belgium). J.H. and J.R. are grateful to the Institute for Science and Technology (IWT) for granting her a doctoral fellowship.

References and Notes

(1) Vinckier, C.; Christiaens, P. *Bull. Soc. Chim. Belg.* **1992**, *101*, 10.
(2) Vinckier, C.; Christiaens, P.; Hendrickx, M. In *Gas-Phase Metal Reactions*; Fontijn, A., Ed.; Elsevier: Amsterdam, 1992; p 57.
(3) Vinckier, C.; Remeysen, J. *J. Phys. Chem.* **1994**, *98*, 10535.
(4) Vinckier, C.; Helaers, J. *J. Phys. Chem. A* **1998**, *102*, 8333.
(5) Vinckier, C.; Christiaens, P. *J. Phys. Chem.* **1992**, 96, 2146.
(6) Vinckier, C.; Christiaens, P. *J. Phys. Chem.* **1992**, 96, 8423.
(7) Vinckier, C.; Helaers, J.; Remeysen, J. *J. Phys. Chem.* **1999**, *103*, 5328.
(8) Plane, J. M. C. In *Gas-Phase Metal Reactions*; Fontijn, A., Ed.; Elsevier: Amsterdam, 1992; p 29.
(9) Plane, J. M. C.; Nien, C. F. *11th International Symposium on Gas Kinetics*, Assisi Italy, September 1990; p O13.
(10) Kashireninov, O. E.; Manelis, G. B.; Repka, L. F. *Russ. J. Phys. Chem.* **1982**, *56*, 630.
(11) Ottinger, Ch.; Zare, R. N. *Chem. Phys. Lett.* **1970**, *5*, 243.
(12) Jonah, C. D.; Zare, R. N.; Ottinger, Ch. *J. Chem. Phys.* **1972**, *56*, 263.
(13) Herm, R. R.; Lin, S. M.; Mims, C. A. *J. Phys. Chem.* **1973**, *77*, 2931.
(14) Parrish, D. D.; Herm, R. R. *J. Chem. Phys.* **1971**, *54*, 2518.
(15) Herschbach, D. R. *Adv. Chem. Phys.* **1966**, *10*, 319.
(16) Davis, H. F.; Suits, A. G.; Hou, H.; Lee, Y. T. *Ber. Bunsen-Ges. Phys. Chem.* **1990**, *94*, 1193.
(17) De Jaegere, S.; Willems, M.; Vinckier, C. *J. Phys. Chem.* **1982**, *86*, 3569.
(18) Brouwers, H. Ph.D. thesis, Faculty of Science, K.U. Leuven, 1984.
(19) *S.A.S. Statistical Package*; S.A.S. Institute Inc.: Cary, NC, 1989.
(20) Fontijn, A.; Felder, W. In *Reactive Intermediates in the Gas-Phase, Generation and* Monitoring; Setser, W., Ed.; Academic Press: New York, 1979; p 59.
(21) Vinckier, C.; Corthouts, J.; De Jaegere, S. *J. Chem. Soc., Faraday Trans. 2* **1988**, *84*, 1951.
(22) Howard, C. J. *J. Phys. Chem.* **1979**, *83*, 3.
(23) Vinckier, C.; Vanhees, I. *J. Phys. Chem.* **1998**, *102*, 1349.
(24) JANAF Thermochemical Tables. *J. Phys. Chem. Ref. Data* **1985**, *14* (Suppl. 1).
(25) Warneck, P. *Chem. Phys. Lett.* **1969**, *3*, 532.
(26) Wagner, O. E. *Bull. Am. Phys. Soc.* **1968**, *13*, 1395.
(27) Herbst, E.; Patterson, T. A.; Lineberger, W. C. *J. Chem. Phys.* **1974**, *61*, 1300.
(28) Grimsrud, E. P.; Caldwel, G.; Chowdhury, S.; Kebarle, P. *J. Am. Chem. Soc.* **1985**, *107*, 4627.
(29) Gislason, E. A. In *Alkali Halide Vapors*; Davidovits, P., McFadden, D. L., Ed.; Academic Press: New York, 1979; p 415.
(30) Maitland, G. C.; Rigby, M.; Smith, E. B.; Wakeham, W. A. *Intermolecular Forces, their Origin and Determination*; Clarendon Press: Oxford, 1987.
(31) *Handbook of Chemistry and Physics*, 73rd ed.; CRC Press: Boca Raton, 1992−1993.
(32) Herzberg, G. *Molecular Spectra and Molecular Structure*; Krieger Publishing Company; Malabar, Florida, 1991; Vol. III, p 602.
(33) Smith, I. W. M. *Kinetics and Dynamics of Elementary Gas Reactions*; Butterworths: London, 1980.